

The infrared spectrometer for Twinkle

Martyn Wells,
UK Astronomy Technology Centre, Edinburgh, Scotland UK

Twinkle is a small satellite mission to observe the atmospheres of exoplanets in the visible to near infrared. This paper describes the design of the infrared (1.3 to 4.5 micron) spectrometer which works at the diffraction limit of the 450mm diameter telescope and at a resolving power of 300 (1.3-2.4 microns) and, in order to achieve the required SNR, $R=30$ for 2.4-4.5 microns. The planetary spectrum is obtained by taking differences between the spectra of star + planet at different phases of the planet's orbit so there is an emphasis of spectral and radiometric stability. The design incorporates a number of features to enhance this stability

- compact all aluminium structure and mirror substrates to reduce alignment offsets when cooled to the operating temperature of $\sim 100\text{K}$

- pupil imaging in the across dispersion direction to minimise changes due to sub-pixel variations in sensitivity and reduce the number of illuminated pixels for background measurements

Keywords: Exoplanets, Space telescopes-IR, Innovative space telescopes and technologies.

1. INTRODUCTION

The Twinkle satellite project is described in a paper in this conference [Savini, G. et al 2016, hereafter Paper1]. It will have a science payload consisting of a 450mm diameter telescope, visible spectrometer, fine guidance system and Near Infrared Spectrometer. This paper describes the opto-mechanical design of the NIR spectrometer and how the challenging requirements on stability, both radiometric and spectroscopic, are addressed. The detailed science requirements for this instrument are given in Paper 1, and flow down to the NIR spectrometer as per Table 1.

Similar small low resolution NIR spectrometers [Wells, M. 1990, Houck, J.R. et al 2004] have been flown successfully on space based observatories. They use all aluminium optics and supporting structures which provide good homologous contraction, that can be accurately modelled, when cooled to cryogenic temperatures and good alignment stability during operations. Similar all aluminium construction methods are also used on numerous ground based IR cryogenic instruments and for larger space instruments such as MIRI on the JWST [Wells, M., et al 2015]. Building on this heritage the Twinkle NIR spectrometer is also all aluminium apart from 2 prisms used to split the wavelength range and as the dispersion element in the longer wavelength channel. It observes the target star/planet and background adjacent to the star in separate apertures over the wavelength range 1.3 to $4.5\mu\text{m}$

1.1 NIR Spectrometer Requirements

The main science requirements for the NIR instrument are listed in Table 1. Additionally the spectrometer is required to operate at cryogenic temperatures (100K) and to have high radiometric and spectroscopic stability.

2. OPTICAL DESIGN OF THE INFRARED INSTRUMENT

The IR instrument is split functionally into 5 sections.

1. Dichroic splitting of the light into the 2 channels 1.3 – $2.42\mu\text{m}$ and $2.42 - 4.5\mu\text{m}$ and for each channel
2. Apertures to control background in the stellar spectra and to define the background sampling areas
3. Collimation of the beams
4. Dispersion
5. Imaging of the spectra on to the common detector

Table 1. Basic NIR spectrometer requirements

	Parameter	Value	Unit	Comment
Science requirements	IR channel Wavelength range	1.3 – 4.5	μm	Split into 2 bands 1.3 – 2.42 μm and 2.42 – 4.5 μm
	Resolving power	300 70		< 2.4 μm > 2.4 μm
	Detector background area	10 x area of the star aperture		In two adjacent strips of sky
	Operating temperature	100	K	
Interface requirements	Primary mirror diameter	450	mm	
	Telescope output f/ratio	11.46		
	Telescope exit pupil location	261	mm	Before focus
	Detector pixel size	15	μm	
	Detector format	1280 x 1024	pixels	

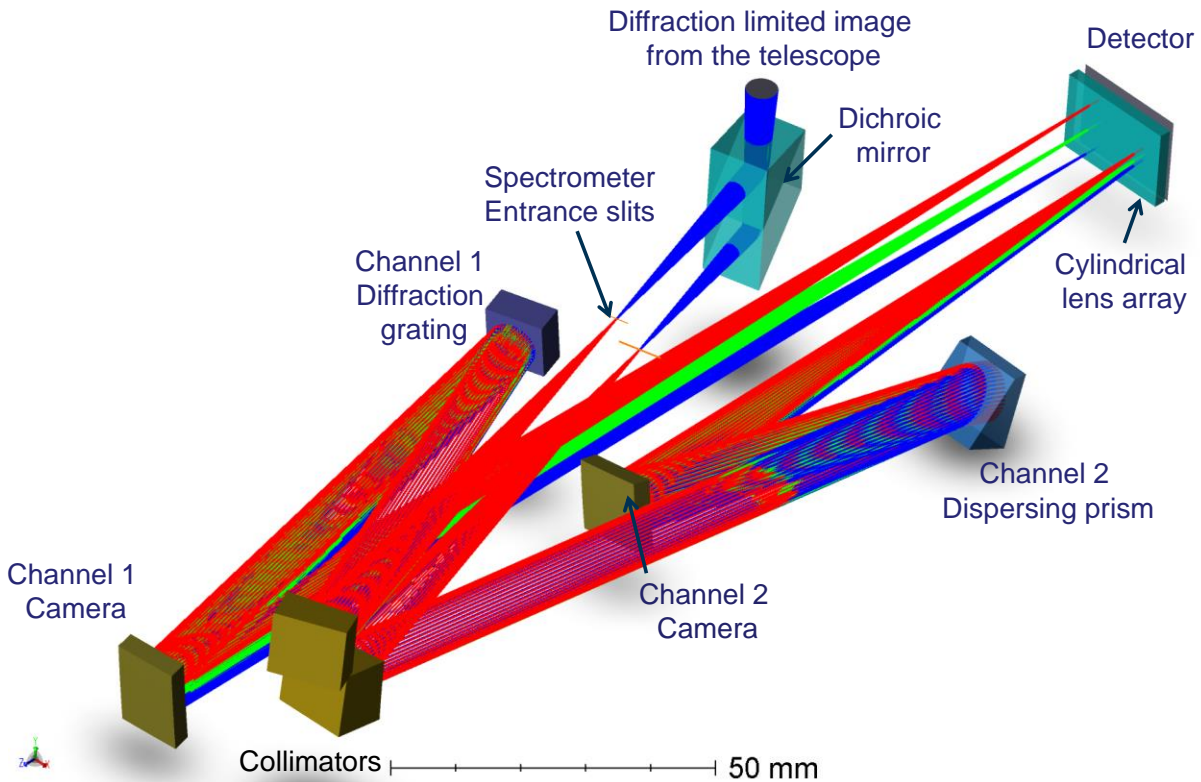


Figure 2-1. Perspective view of the IR instrument with the "entrance" prism seen in the top centre of the picture. The rays enter vertically from the top and the two outputs (reflected and transmitted in the prism) exit the prism towards the bottom left of the viewer. The multitude of rays seen encompass the three wavelengths per channel and the centres of the 3 fields (star + background fields on both sides of the star).

2.1 Overall optical layout

This functionality is provided by two spectrometers which are intricately connected even though they only share two common optical elements (dichroic beamsplitter and detector) within the instrument (after the telescope optical train). The spectrometers work with the diffraction limited image delivered by the telescope and cover two spectral bands, 1.3-2.42 μm and 2.42-4.5 μm with resolving powers of $R=300$ and $R=70$ respectively. They also provide separate, simultaneous, measurements of the background spectra along 2 slits next to the target star. A picture of the overall design and ray-tracing can be seen in Figure 2-1 albeit a full set of projections is needed to fully appreciate the propagation of rays through the optical system starting from the prism beam-splitter and ending on a common detector.

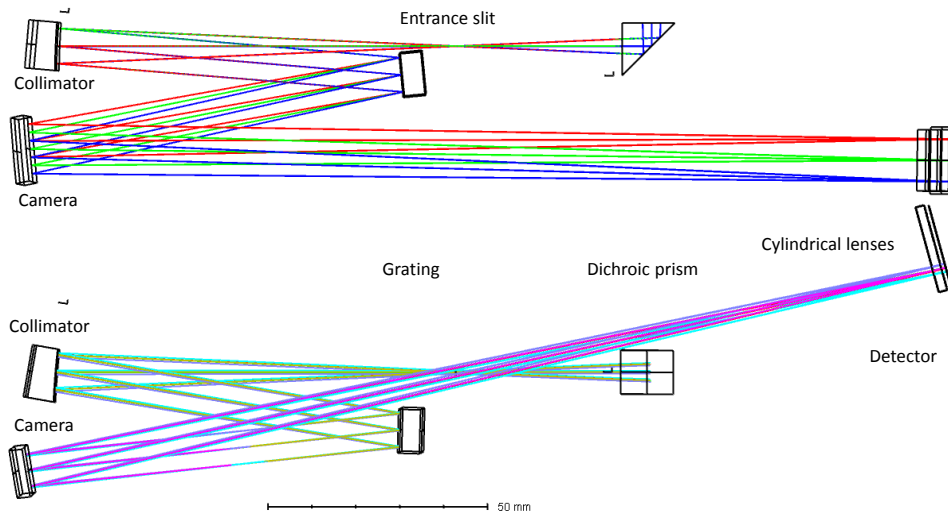


Figure 2-2. Channel 1 - Elevation (top) and Plan (bottom) view. (Top) Different colours represent different wavelengths. (Bottom) different colours represent the different fields in the sky.

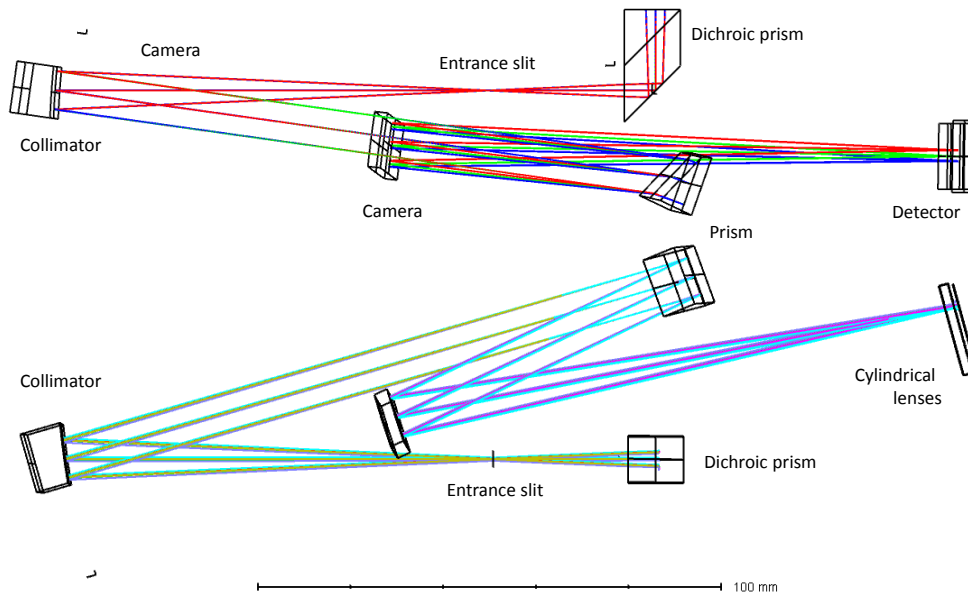


Figure 2-3. Channel-2 - Elevation (top) and Plan (bottom) view. (Top) Different colours represent different wavelengths. (Bottom) different colours represent the different fields in the sky.

The same architecture can be viewed in Figure 2-2 and Figure 2-3 where the two channels have been separated and shown in projection views for clarity. The two projections are referred to as “Plan” and “Elevation”. The latter being the dispersion plane where the separation of rays caused by the diffraction grating causes the spectrum to spread on the image plane and the former the “spatial” plane where the background fields are separated from the central star field and where cylindrical lenses in front of the detector image the pupil on to the detector in this plane.

The two layouts have been checked for non-invasive presence of optical elements in each other’s beams. The instrument envelope is enclosed in an instrument box that interfaces to an optical bench on the back of the telescope. Within this instrument box, a few sectors are defined in order to increase the level of stray-light rejection (already small given the slit-mask input).

These sectors are identified as and illustrated in Figure 2-4:

- Main IR-Instrument Box: the entire volume within the instrument box to which all IR instrument components are mounted and that provides the main interface to the optical bench.
- The “Enclosed Instrument Box” which is essentially most of the above with the exclusion of the dichroic prism which is left outside given that the most stringent aperture control can be exercised at the slit-mask.
- The inner detector compartment which a box which can be used to control the thermal emission impacting on the detector from directions other than that of the optical train. As can be seen in Figure 2-2Figure 2-3 there is an area 50mm in front of the detector clear of optical components. This space can be used for a rectangular baffle that restricts the thermal emission from the instrument housing reaching the detector. This baffle is indicated in Figure 2-4

A stiff optical board will be produced in an ‘L’ configuration (base and left hand wall), shown in green in Figure 2-4. This will be used to mount aluminum diamond turned fold mirrors and diffraction grating. The prisms will be held in kinematic mounts by sprung loaded clamps on posts. All the structure and mirrors and the directly ruled grating will be manufactured using the same aluminium alloy and alignment is achieved using sacrificial shims which ensures that distortions on cooling will be small and within requirements.

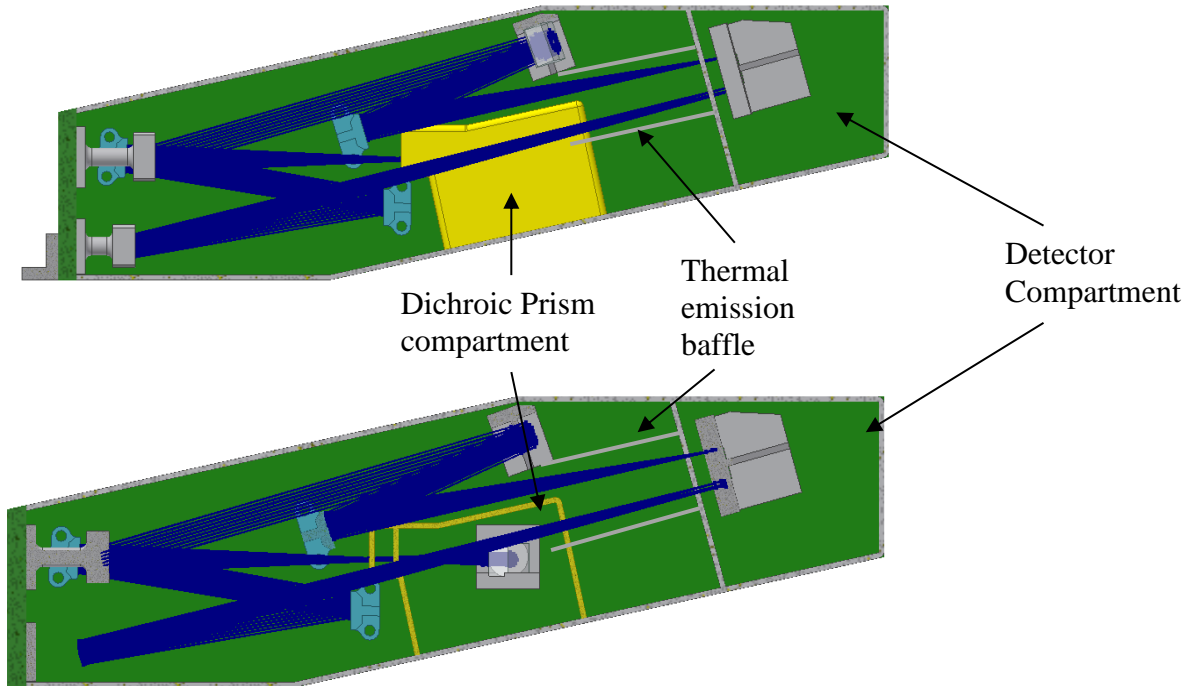


Figure 2-4 Top and bottom views of the mechanical model showing compartments within the main enclosure.

2.2 End to end optical description

We now describe the elements of the IR instrument as we follow the light path in the instrument.

The telescope delivers a diffraction limited ($\lambda \geq 1.3 \mu\text{m}$) $f/11$ beam with its exit pupil 260 mm in front of the focus. This beam is intercepted by the dichroic prism that splits the light into Channel 1 (1.3 to $2.42 \mu\text{m}$) and Channel 2 (2.42 to $4.5 \mu\text{m}$) – see Figure 2-5 below.

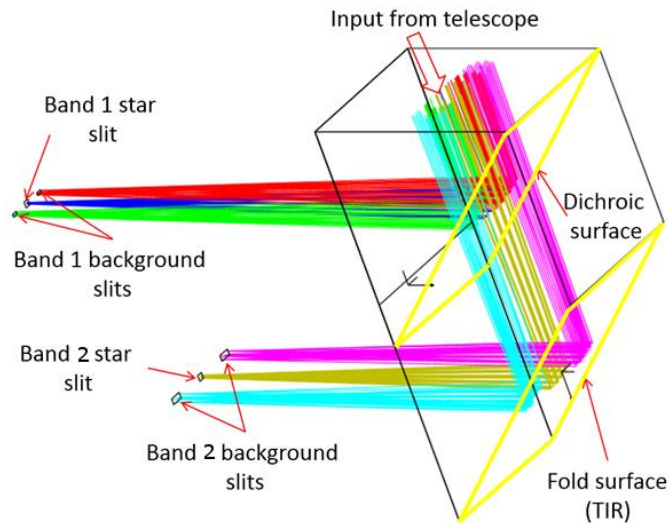


Figure 2-5 A Calcium Fluoride Prism beam-splitter with a dichroic coating deposited on the intermediate surface acts as a wavelength separator reflecting the short wavelength input and transmitting the longer wavelength channel.

This prism consists of 2 separate CaF₂ prisms, one with a right angled isosceles cross-section and the other a parallelogram. The dichroic coating is placed at the common face. In practice there will be a spectral transition region for this coating so the spectral range of each channel will need to extend above (Channel 1) and below (Channel 2) $2.42 \mu\text{m}$. The detector has sufficient pixels in the dispersion direction to accommodate these band extensions. The wavelengths $>2.42 \mu\text{m}$ are reflected by the lower face of the 2nd prism by total internal reflection. The image of the star and sky is formed just beyond this prism with the two channels separated by 12mm. The alignment and alignment stability of the stellar images at the entrance apertures of the spectrometers is critical to the radiometric stability. The calibration of the guidance system can be achieved on one channel or an average of the two using, for example, a peaking up routine. But the co-alignment of the two apertures is dependent on the mounting of the apertures and the beamsplitter. Therefore care will be taken to ensure a short, mechanically stable path between the mount of the prism and the mount of the slits.

There are spectrometer slit masks in each channel that act to limit the background flux entering the spectrometer. For light from the star and associated planet(s) the PSF is the effective slit width while for the background the physical width of the slit is used. These slit widths combined with dispersing element, collimator and camera mirrors and detector pixels determine the spectral resolving power. It is important that small movements of the star caused by telescope jitter do not significantly affect signal reaching the detector. To achieve this the aperture shown in Figure 2-6 is used; placing the edge of the aperture at the 1st dark ring of the Airy PSF minimises changes of transmitted flux with movement of the star because the signal at the edge is a minimum as is the radial differential. For the star the PSF width is proportional to wavelength so the resolving power is constant and the sampling increases with wavelength. For the background the opposite applies – resolving power increases with wavelength, sampling is constant. The angular and linear sizes of the

slits are given in Table 2. The separation of the background slits is such that light from either of them does not fall on the detector at the location of the stellar spectrum. The length of the slits is determined by the available area of the detector, this is 60arcsec for Channel 1 and 112arcsec for Channel 2. The slit mask also represents the only access to an enclosed area which effectively shields most of the instrument from stray light reducing the constraints on the telescope baffle.

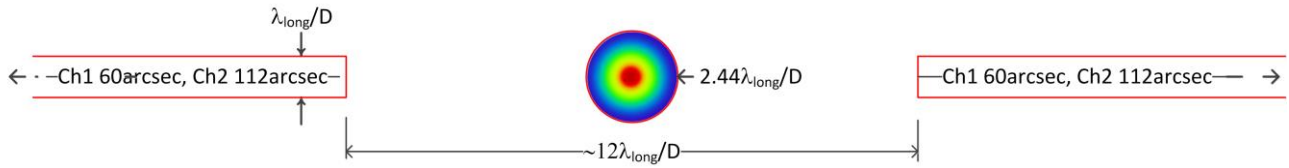


Figure 2-6 Entrance slit for the two spectrometers. The circular area around the star is $2.44\lambda/D$ in diameter at the longest wavelength in each channel. The width of the background slit is λ/D also at the longest wavelengths in each channel. The distance from the centre of the star to the inner edge of the background slit is 13 arcsec for Channel 1 and 24 arcsec for Channel 2.

Table 2 The Airy PSF angular and linear sizes at the instrument entrance slit.

Wavelength	$2.44 \lambda/D$	Linear size at slit	λ/D	Linear size at slit
μm	arcsec	mm	arcsec	mm
1.3	1.45	0.036	0.60	0.015
2.4	2.68	0.067	1.10	0.027
4.5	5.03	0.126	2.06	0.051

The beams leaving the 2 entrance slits are collimated by 2 diamond turned mirrors which in turn direct light towards the dispersing elements, a diffraction grating for Channel 1 and a calcium fluoride prism for Channel 2. The spectra are then imaged on to the detector by 2 more diamond turned mirrors.

The spectra are aligned to lie along columns of pixels by rotating the grating/prism about their optical axes. The sampling of the spectra is set by imaging the FWHM (λ/D) at the shortest wavelength in each spectrometer (1.3 and $2.4\mu\text{m}$ for Ch1 and Ch2 respectively) onto 2.5 pixels. This is equivalent to imaging the 1st dark ring diameter onto 6 pixels. The resolving power and length of the spectra are then set by the dispersion in each channel.

Detector arrays such as those proposed for Twinkle can present a variation in the QE (gain) at the sub-pixel level. This means that jitter in the star position along the entrance slit can result in appreciable changes in signal level. To reduce this effect an array of cylindrical lenses is placed in front of the detector that, in the cross-dispersion direction, image the telescope pupil onto the detector. This means that the movement of the star at the instrument entrance focal plane is translated into a change of angle of incidence at the detector which results in a smaller change in signal than a direct lateral shift.

Another advantage of these cylindrical lenses is that the background (with a signal \ll stellar signal) is concentrated into a number of narrow spectra which improves the SNR because of the smaller number of pixels contributing to the dark current and read noise.

These lenses are silicon, 1mm wide, and can be manufactured via standard etching techniques on a single substrate which can then be anti-reflection coated for the respective bands.

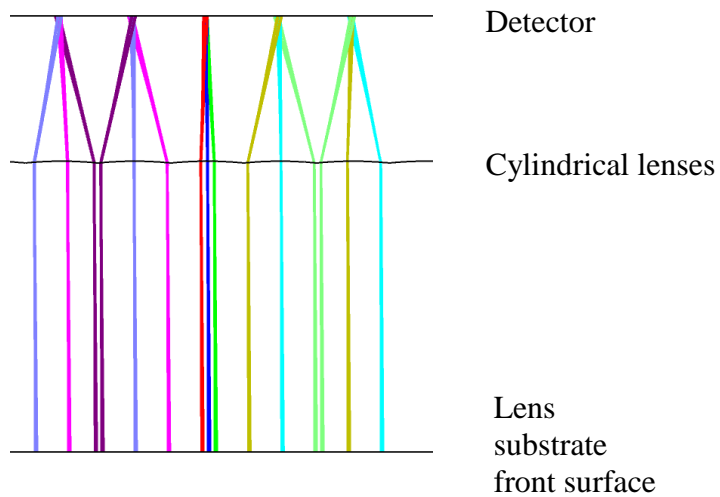


Figure 2-7 Cylindrical lenses showing star in the centre (blue centre, red and green $\pm 1.22\lambda/D$) and 5 sections of background.

Figure 2-7 illustrates how the cylindrical lenses work. The blue red and green beams represent positions at the centre of the star and at $\pm 1.22\lambda/D$. At the surfaces of the lens these beams are separated and without the cylindrical surface they would intercept the detector with a spacing of 6 pixels. The cylindrical surface converges them onto a pupil image at the detector.

3. OPTICAL PERFORMANCE

Figure 3-1 shows the geometric footprints in Channel 1 for 5 sources placed at the centre and at 90deg intervals around the circumference of a $1.22\lambda/D$ circle where in this case is $2.4\mu\text{m}$. This shows the cross-dispersion sources (red and green) fall on top of the centre blue source whereas the sources in the dispersion direction are at ± 5 pixels.

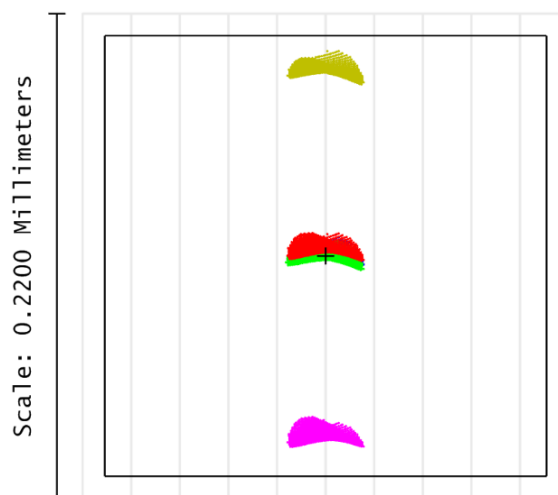


Figure 3-1 The geometric footprint for point sources placed at the centre of the star and at $\pm 1.22\lambda/D$ in both Y (dispersion) direction and X(cross-dispersion).

The adjacent lens shows how the background is imaged. As can be seen for sources at the edge of this lens the light in the background portion of the slit is not concentrated onto one position. To find out what the concentration is an extended source which covered the width of a lens was placed at the telescope entrance, the results are shown in Figure 3-2.

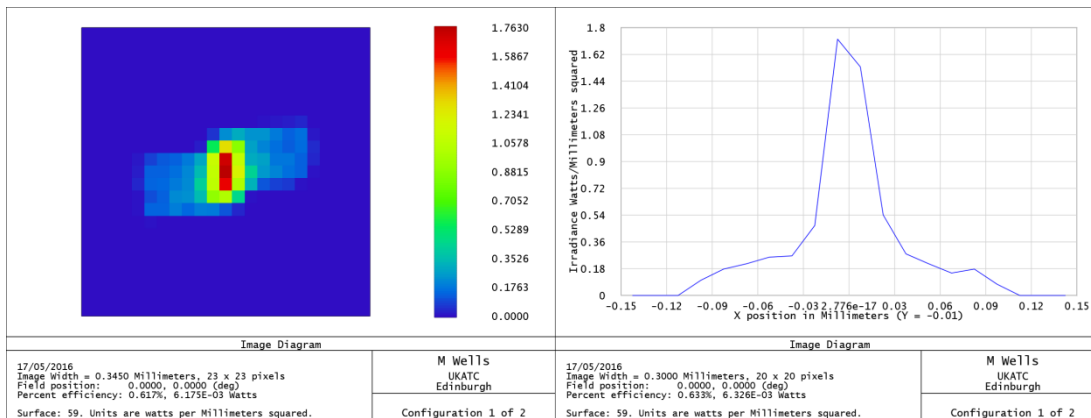


Figure 3-2 Geometric concentration of the background light.
Left 2D plot showing the height of the slit and the spread of light.
Right Cross-section showing most of the light is concentrated into a strip 4 pixels wide.

The diagrams in Figure 2-7, Figure 3-1, Figure 3-2 are for geometric raytracing which serves to fix the sampling and dispersion of the images. But the system works at the diffraction limit so analysis that takes this into account is needed to obtain the PSFs that can be used in sensitivity analyses. For the low, centre and high wavelengths in each channel the Huygens PSF modelling facility in Zemax was used to obtain the PSFs shown in Figure 3-3. The PSFs increase in size with wavelength in both the spectral and spatial directions. The increases are as expected for the spectral directions in both channels and the spatial direction in Channel 2. However for the spatial direction in Channel 1 the increase is greater than expected which can be seen in Figure 3-4 and Figure 3-5 which shows the spatial and spectral cross-sections for the Channel 1 and Channel 2 PSFs. Close inspection of the raytracing for Channel 1 indicates that this larger than expected increase in the Channel 1 spatial PSF width is caused by the axial position of the pupil image changing with wavelength so as to give the larger spatial PSF width compared to the spectral PSF width. More control of the PSF widths can be achieved using toroidal camera mirrors which can independently image slit and pupil at the detector.

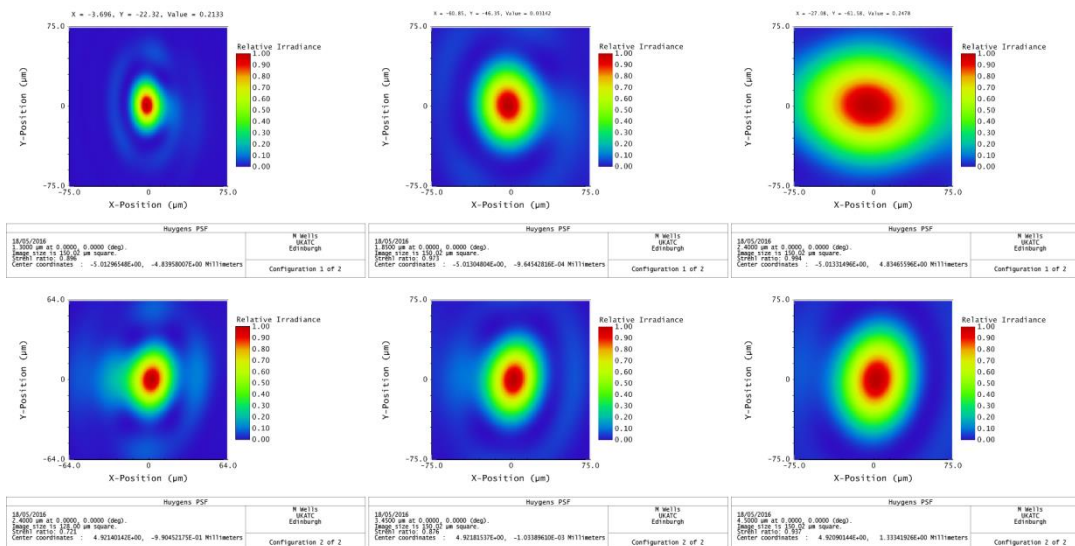


Figure 3-3 PSFs for Channel 1 (top row) at 1.3µm, 1.85µm and 2.4µm and Channel 2 (bottom row) at 2.4µm, 3.45µm and 4.5µm. The box is 10x10 pixels for all the PSFs.

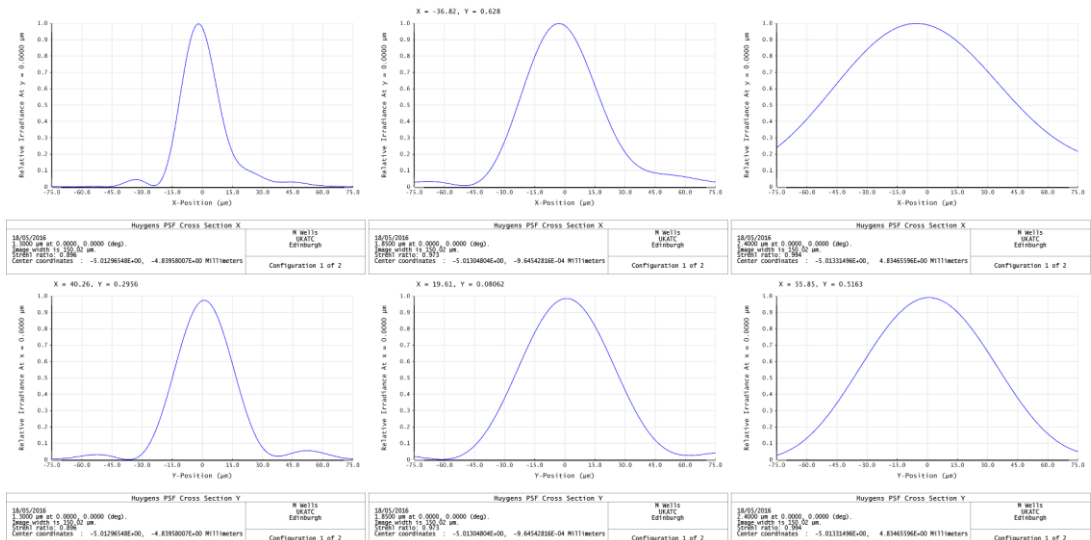


Figure 3-4 Channel 1 PSF cross-sections. Top – spatial Bottom –spectral. Vertical grid lines at 1 pixel intervals

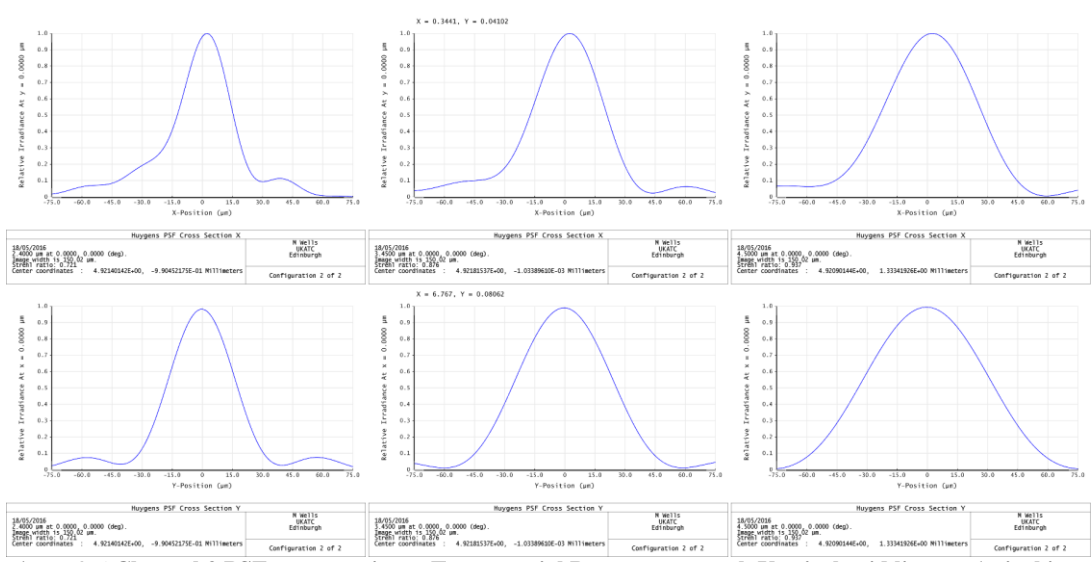


Figure 3-5 Channel 2 PSF cross-sections. Top – spatial Bottom –spectral. Vertical grid lines at 1 pixel intervals

3.1 Optical Transmission

The optical transmission for the 2 channels is estimated as follows

1. Mirrors. The coating on the mirrors will be enhanced silver; there are 5 telescope mirrors and 2 spectrometer mirrors per channel, the collimating and camera mirrors. The reflectivity of enhanced silver for $\lambda > 1.3 \mu\text{m}$ is taken to be 0.98 based on manufacturers values > 0.985 and making an allowance for contamination. The transmission for the 7 mirrors is 0.87
2. The dichroic and dispersing prisms are CaF_2 which have a reflectance of 3% at each glass/air interface. These will be uncoated so the transmission of the dichroic prism will be 0.94.

The dispersing prism is used in double pass so there are 2 glass/air interfaces $T=0.94$. In addition the rear surface is silver coated $T=0.98$.

The transmission and reflectivity of the dichroic coating are estimated from manufacturer standard curves to be $T > 0.9$, $R > 0.9$.

3. For both channels the cylindrical lens will be AR coated on both sides. This lens is high refractive index silicon. T=0.95 assumed for AR efficiency giving overall transmission for this component T=0.90

4. For Channel 1 the grating efficiency can be taken as 65% minimum - experience from MIRI and modeling done for other instruments.

$$\text{Channel 1 overall transmission } 0.87 \times 0.9 \times 0.94 \times 0.9 \times 0.65 = 0.43$$

$$\text{Channel 2 overall transmission } 0.87 \times 0.9 \times 0.94 \times 0.9 \times 0.94 \times 0.98 = 0.61$$

3.2 Optical Transmission

The cylindrical lens array produces a number of spectra on the detector, one in each channel for the star and 3 either side of them from the background slits. This is illustrated in Figure 3-6. This image shows the low, mid and high wavelengths as indicated for Channel 1. The shorter spectra in channel 2 result from the lower dispersion of the prism compared to grating and results in a resolving power of about 70.

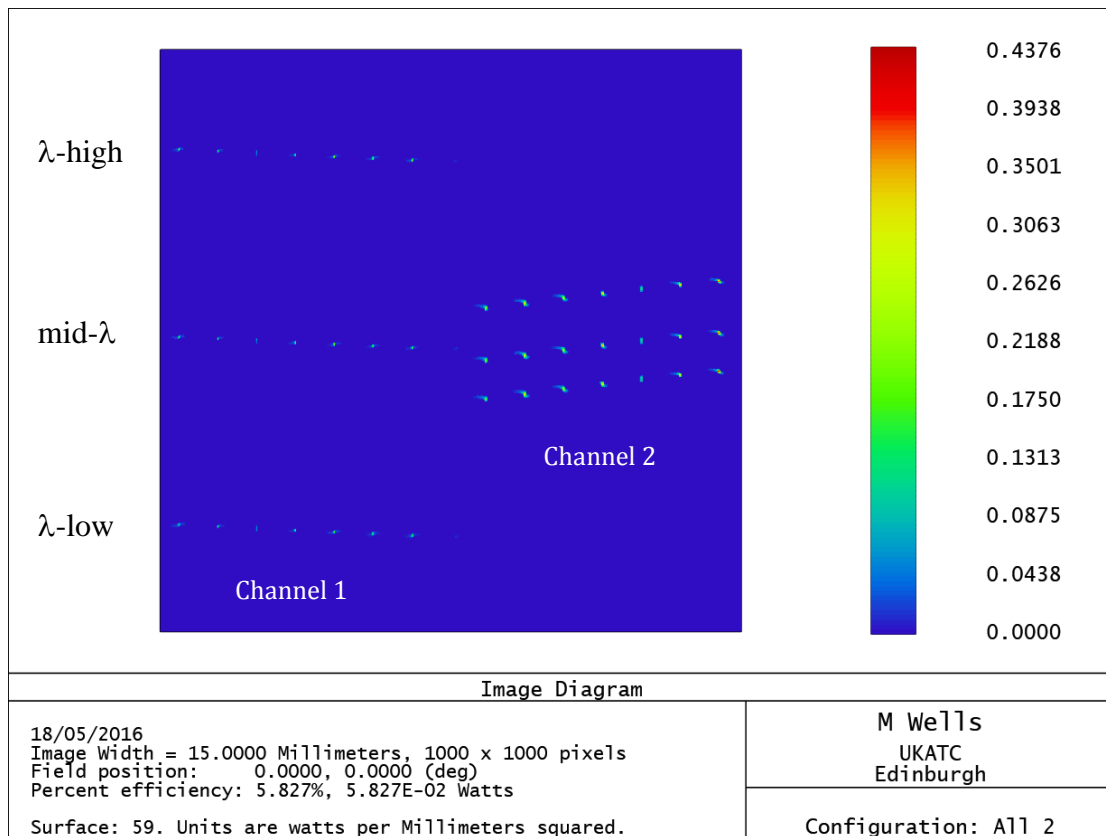


Figure 3-6 Format of spectra on the detector

4. CONCLUSION

This paper describes a dual spectrometer that fulfills the requirements placed on it by the science case in Paper 1. It uses an all aluminium construction for alignment stability on cooling, a novel cylindrical lens array to minimize signal changes caused by pointing jitter and is compact enough to meet the thermal and mass limits imposed from the chosen spacecraft.

5. ACKNOWLEDGEMENTS

I wish to acknowledge the lively discussion, critique and appreciation of this work by my Twinkle colleagues at University College London – Giovanna Tinetti, Marcell Tessenyi and Giorgio Savini, at Cardiff University - Enzo Pascale at RAL – Ian Tosh.

REFERENCES

- [1] Savini, G. et al, TWINKLE – A Low Earth Orbit Visible and Infrared Exoplanet Spectroscopy Observatory, *Proc. SPIE* 9904, Space Telescopes and Instrumentation 2016, (2016)
- [2] Wells, M., "ISOPHOT-S: a low-resolution, near-infrared spectrometer for ISO", *Proc. SPIE* 1235, Instrumentation in Astronomy VII, 911 (1990)
- [3] Houck, J.R. et al, "The infrared spectrograph on the Spitzer Space Telescope", *Proc. SPIE* 5487, Optical, Infrared, and Millimeter Space Telescopes, 62 (2004)
- [4] Wells, M., et al, The Mid-Infrared Instrument for the James Webb Space Telescope, VI: The Medium Resolution Spectrometer, *PASP* 127:646-664, 2015 July